Water Science & Technology

IWA PUBLISHING

Water Science & Technology Vol 87 No 11, 2776 doi: 10.2166/wst.2023.169

Effects of electrochemical intervention on the remediation of black-odorous water: insights into microbial community dynamics and functional shifts in sediments

Yingying Shi[a,b], Zhipeng Wei[a,b], Yaofei Xu[a,b], Xiang Lu[c] and Aidong Ruan[a,b,*]

[a] State Key Laboratory of Hydrology-Water Resources and Hydraulic Engineering, Hohai University, Nanjing 210098, China
[b] College of Hydrology and Water Resources, Hohai University, Nanjing 210098, China
[c] Department of Biosciences, Centre for Biogeochemistry in the Anthropocene, University of Oslo, Oslo 0316, Norway
*Corresponding author. E-mail: adruan@hhu.edu.cn

AR, 0000-0002-2076-4660

ABSTRACT

Black-odorous water is a severe environmental issue that has received continuous attention. The major purpose of the present study was to propose an economical, practical, and pollution-free treatment technology. In this study, the *in situ* remediation of black-odorous water was conducted by applying different voltages (2.5, 5, and 10 V) to improve oxidation conditions of the surface sediments. The study investigated the effects of voltage intervention on water quality, gas emissions, and microbial community dynamics in surface sediments during the remediation process. The results indicated that the voltage intervention can effectively increase the oxidation–reduction potential (ORP) of the surface sediments and inhibit the emissions of H_2S, NH_3, and CH_4. Moreover, the relative abundances of typical methanogens (*Methanosarcina* and *Methanolobus*) and sulfate-reducing bacteria (*Desulfovirga*) decreased because of the increase in ORP after the voltage treatment. The microbial functions predicted by FAPROTAX also demonstrated the inhibition of methanogenesis and sulfate reduction functions. On the contrary, the total relative abundances of chemoheterotrophic microorganisms (e.g., *Dechloromonas*, *Azospira*, *Azospirillum*, and *Pannonibacter*) in the surface sediments increased significantly, which led to enhanced biochemical degradability of the black-odorous sediments as well as CO_2 emissions.

Key words: black-odorous water, methanogenesis, microbial community dynamics, oxidation–reduction potential, sulfate reduction, voltage intervention

HIGHLIGHTS

- Voltage intervention contributes to the remediation of black-odorous water.
- Applied voltages can effectively improve the oxidation conditions in the sediments.
- Voltages significantly inhibited the emissions of H_2S, NH_3, and CH_4 from sediments.
- Relative abundances of methanogens and sulfate-reducing bacteria decreased at 10 V.
- Abundances of chemoheterotrophic microorganisms increased with increasing voltage.

GRAPHICAL ABSTRACT

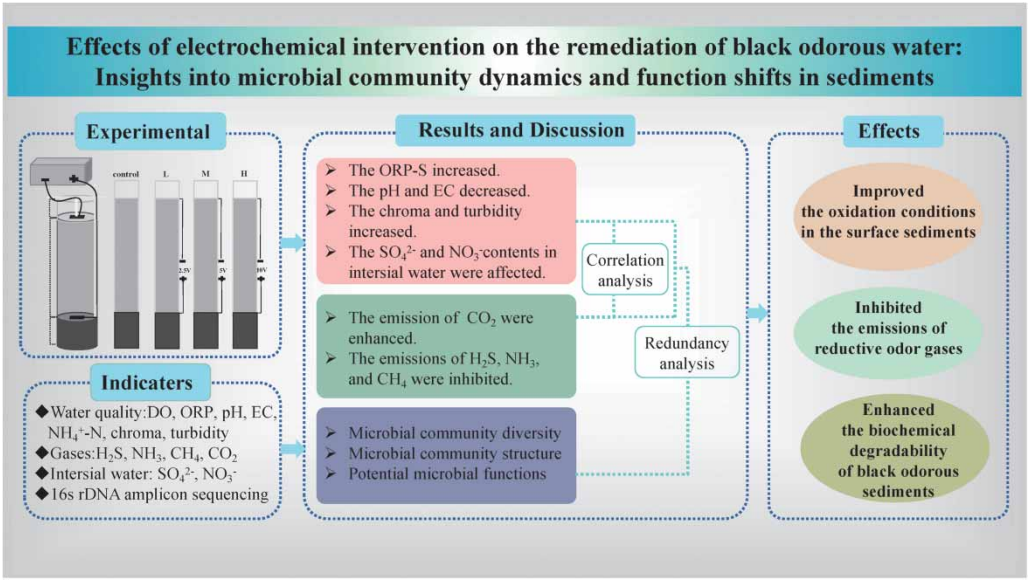

1. INTRODUCTION

Black-odorous water refers to water bodies with black or blackish color and terrible smells, which is an extreme manifestation of water pollution caused by urbanization (Chen *et al.* 2022). This phenomenon has been reported worldwide both in developing and developed countries, such as the St. Johns River in the United States, the Kanda River and the Shakujii River in Japan, the Siak River in Indonesia, and the Nanfei River in China (Cao *et al.* 2020). According to a previous report in September 2019, there are 2,100 black-odorous water bodies in China, of which 71% are distributed in relatively economically developed and densely populated cities in southeast China (Cao *et al.* 2020). The black-odorous phenomenon not only threatens the aquatic ecology but also seriously affects the daily life of the people. Therefore, it has aroused considerable interest among government agencies and academic researchers.

Black-odor is generally observed in extremely contaminated water bodies. The oxidation–reduction potential (ORP) is considered a key factor leading to the occurrence of the black-odorous phenomenon (Chen *et al.* 2020). A large number of pollutants enter water bodies, resulting in a rapid decrease in dissolved oxygen (DO) and a concomitant decrease in ORP (Liu *et al.* 2015). When the ORP in the sediments is lower than −50 mV, anaerobic microorganisms, such as sulfate-reducing bacteria (SRB), methanogens, fungi, and actinomycetes, dominate the microbial community structure (Chen *et al.* 2020). In particular, SRBs are capable of reducing sulfate to S^{2-} and H_2S under anaerobic conditions, both of which are critical compounds for black-odor formation (Wang *et al.* 2014; Liu *et al.* 2015; Song *et al.* 2017). Extensive research has shown that S^{2-} plays an important role in the water blackening process (Wang *et al.* 2014; Song *et al.* 2017). The prevalent odors such as NH_3, H_2S, and volatile organic sulfur compounds (VOSCs) are produced during the anaerobic decomposition of sulfur-containing organics (Song *et al.* 2017). Moreover, odorous substances such as geosmin and 2-methylisoborneo-l (2-MIB) are produced during the metabolism in fungi and actinomycetes, which may aggravate the odor in water (Watson 2003). In addition, dimethyl trisulfide (DMTS) and β-ionone released during the algal decomposition process are the sources of odor in algae-induced black-odorous water (Wang *et al.* 2014).

Over the past century, national and international researchers have conducted several research studies on the treatment of black-odorous water (Cao *et al.* 2020). Traditionally, black-odorous water treatment methods mainly include sediment dredging (Liu *et al.* 2015), artificial aeration (Pan *et al.* 2016), chemical methods (Liu *et al.* 2016), and biological methods (Yuan *et al.* 2018). Although sediment dredging and artificial aeration can rapidly reduce the pollution loads and increase DO, they are not permanent solutions and can easily lead to the transfer of pollutants from sediments to overlying water. The chemical methods can rapidly improve water transparency and eliminate odors, but the additional treatment techniques for residual sludge can increase economic costs. Even though the studies have demonstrated the ability of some microorganisms to

degrade pollutants efficiently, this ability is governed by environmental conditions and have certain ecological risks. Recently, more attention has been paid to electrochemical water treatment technology for its extraordinary features and advantages. The long-term performance of any treatment for the removal of the black-odor depends on the growth and activities of several functional microorganisms. Therefore, more attention should be paid to the microbial community dynamics and functional variations in the treatment systems of black-odorous waterbodies. Electrochemical technology has been applied so far to different types of wastewater treatment, including actual textile wastewater, industrial wastewater, and toilet sewage (Zhang *et al.* 2019). However, few studies have investigated the performance of electrochemical technology in the treatment of black-odorous water. Moreover, little is known about the microbial community dynamics and functional variations during the remediation of black-odorous water with electrochemical intervention. In addition, there is a lack of clarity on the underlying mechanisms of electrochemical intervention affecting the biochemical remediation of black-odorous water.

In this study, DC voltages (2.5, 5, and 10 V) were used to increase the ORP of the surface sediments to accelerate the *in situ* remediation process of black-odorous water. The purpose of this study was: (i) to examine the effects of voltage intervention on the physicochemical properties and gas emissions in black-odorous water; (ii) to analyze the effects of voltage intervention on the microbial community structures and their predicted functions in surface sediments; (iii) to elucidate the underlying mechanisms of the effects of voltage intervention on water quality and odors during the remediation process. The focus of this study was to investigate the performance of electrochemical technology during the remediation of black-odorous water and provide fundamental support for bioelectrochemical water treatment technologies.

2. MATERIALS AND METHODS

2.1. Experimental scheme

In this study, the sediments were collected from the center of Chaohu East Lake, Anhui Province, China. The collected sediments were placed in a ventilated room for drying, crushing, sieving, and mixing for complete homogenization. Tap water was used as the overlying water in each reactor. The physicochemical properties of tap water are shown in Supplementary material, Table S1. The transparent cylinder (inner diameter: 10 cm and height: 100 cm) made up of polypropylene was used as the experimental reactor. The reactor was filled with 20 cm of sediments and a water column of 70 cm. The reactors were kept undisturbed in the laboratory for 3 weeks for the stratification of their soil, water, and microorganisms. The experimental device is depicted in Figure 1(a).

Methionine was selected to induce the black-odorous water formation in this study, as it contains C, N, and S and has the potential to cause a black-odor phenomenon (Lu *et al.* 2012). In total, 645.66 mg of methionine was added in each reactor, such that the concentration of methionine in each reactor was 117.44 mg/L. The water quality parameters and gas emission rates were continuously monitored after the addition of methionine (Supplementary material, Figure S1). Based on the classifications and standards for urban black-odorous water bodies in China (Supplementary material, Table S2), the experiment was started and recorded as day 0 when the water bodies exhibited an evident black-odor (DO < 2 mg/L, ORP < 50 mV, NH_4^+-N > 8 mg/L) (Cao *et al.* 2020).

The experiment reactors were divided into four groups, namely control, L, M, and H, as shown in Figure 1(b), wherein the improvement in the natural water quality of black-odorous water by self-purification was monitored in the control group. The DC voltages of 2.5, 5, and 10 V were applied to the L, M, and H groups, respectively, to monitor the effects of different voltage interventions on the remediation of black-odorous water. Three parallel devices were set up for each experimental group. The voltage-connected reactors were powered using an adjustable DC voltage regulator (MS-305D, Maisheng, China) and copper wires (1.5 mm^2). Graphite electrodes (4 cm $\times$ 4 cm $\times$ 1 mm) were used for the reactors, with the cathode placed on the water surface and the anode placed on the sediment surface. The voltages were applied from 20:00 to 8:00 (the next day) for 12 h daily, which is determined based on the average light hours of natural water bodies.

The overlying water samples and headspace gas samples were collected every 2 days during the experiment. The water samples were collected from the middle zone of the water column using a 5-mL pipette gun, while the gas samples were obtained with a 10-mL plastic syringe after sealing the reactor for an hour. The sediment and interstitial water samples were collected only on days 0, 10, 20, and 30 to avoid disturbing the sediment-water stratification frequently. All the samples were collected in the power-off state. Furthermore, the overlying and interstitial water samples were filtered using a 0.45 μm membrane for subsequent analysis. The freeze-dried surface sediment samples were sent to the Biomarker Technologies Corporation, Beijing, China for high-throughput sequencing on Illumina Novaseq 6000 (Illumina, Santiago, CA, USA).

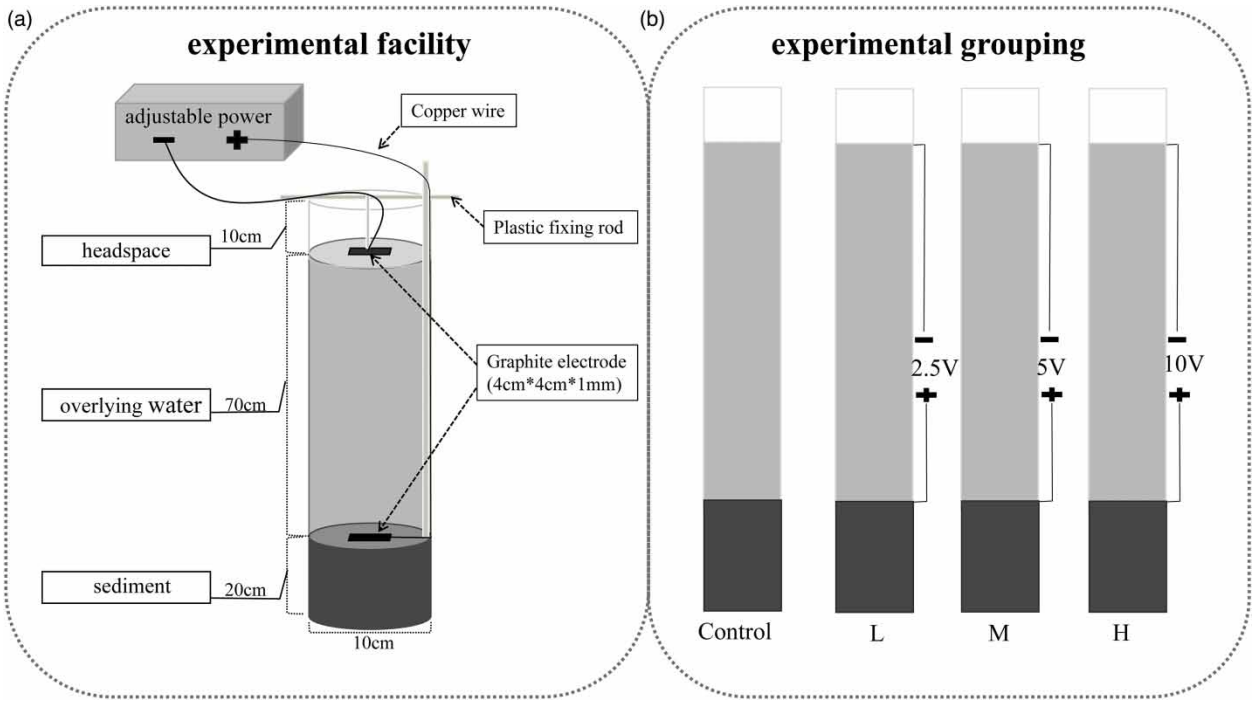

Figure 1 | Experimental device (a) and grouping diagram (b).

2.2. Chemical analysis

The physicochemical characteristics observed in this study included pH, electrical conductivity (EC), DO, ORP of overlying water (ORP-W), ORP of surface sediment (ORP-S), ammonia nitrogen concentration (NH_4^+-N), turbidity, chroma, interstitial sulfate concentration (SO_4^{2-}) and interstitial nitrate concentration (NO_3^-). EC, pH, DO, and turbidity of the water column were measured *in situ* by a multiparameter water quality sonde (YSI 6600, Yellow Spring, USA). ORP was measured using the Unisense Microsensor Monometer (Version 1.0, Unisense, Denmark). The NH_4^+-N concentration of the overlying water was determined by a Multiplate Reader (M2e, Molecular Devices, USA), while chroma was measured using a spectrophotometer (UV-5100, Yuanxi Instrument, China) (Gollnisch *et al.* 2021). The SO_4^{2-} and NO_3^- concentrations in interstitial water samples were determined using ion chromatography (ICS-2000, Dionex, USA). The concentrations of H_2S and NH_3 gas were measured using portable gas analyzers (GT903-F-H_2S/GT903-F-NH_3, Kerno, China). The CH_4 and CO_2 gas concentrations were analyzed using gas chromatography (Trace GC, Themrmo Fisher, USA).

The experimental period was 30 days, during which most indicators, including pH, EC, DO, chroma, turbidity, SO_4^{2-}, NO_3^-, H_2S, NH_3, CH_4 and CO_2, were observed. However, on the 25th day, the Unisense Microsensor Monometer measuring ORP encountered some uncontrollable accidents, rendering it unusable. Consequently, ORP observations were only carried out up to day 25. Moreover, since only a small amount of NH_4^+-N was degraded by the day 30, the observation period for this indicator was extended to 50 days to investigate the effects of voltage interventions on NH_4^+-N degradation. In addition, due to time constraints, the physicochemical analyses and sample collections could not be completed within a single day. Hence, the observation times of the physicochemical parameters and gas emission rates were not entirely consistent.

2.3. High-throughput sequencing

Three parallel samples of the same group at the same sampling time were mixed to account for sediment heterogeneity. DNA was extracted with the TGuide S96 Magnetic Soil/Stool DNA Kit (DP812, Tiangen, Beijing, China) according to the manufacturer's instructions. The concentration of the extracted DNA was tested using NanoDrop and the purity was determined using agarose electrophoresis at a concentration of 1.8%. The 515F (5′-GTGYCAGCMGCCGCGGTAA-3′) and 926R (5′-CCGYCAATTYMTTTRAGTTT-3′) universal primer set was used for the amplification of the V4–V5 hypervariable regions of 16S rRNA gene. The PCR amplicons were purified using VAHTSTM DNA Clean Beads (N411-03, Vazyme, Nanjing,

China) and quantified by the ImageJ software. After the individual quantification step, amplicons were pooled in equal amounts. For the constructed library, Illumina Novaseq 6000 (Illumina, Santiago, CA, USA) was used for sequencing. The raw amplicon sequences were submitted to National Center for Biotechnology Information (NCBI) (BioProject ID: PRJNA901879; BioSamples ID: SAMN31736351–SAMN31736366).

2.4. Bioinformatics analysis

The bioinformatics analysis in this study was performed using the BMK Cloud (www.biocloud.net). The raw data obtained were primarily filtered by Trimmomatic (version 0.33). The identification and removal of the primer sequences were processed by Cutadapt (version 1.9.1). The clean reads obtained from the previous steps were assembled by USEARCH (version 10). The dada2 method in QIIME2 software was used for denoising and removal of chimera sequences for obtaining amplicon sequence variants (ASVs) (Callahan *et al.* 2017). Taxonomy annotation of the ASVs was based on the Naive Bayes classifier in QIIME2 using the SILVA database. The microbial community structures at phylum and genus levels were represented by plotting stacked histograms using OriginPro. The distribution of dominant genera across four groups was analyzed using the Cytoscape network analysis. The alpha diversity indices (Chao1, Ace, Shannon index, and Simpson index) were calculated by QIIME2. The beta diversity was determined for evaluating the similarity of microbial communities in different samples. Principal component analysis (PCA) was performed to analyze the beta diversity by Chiplot (www.chiplot.online). The microbial functional profiles were predicted using FAPROTAX. The functional clustering heatmap was constructed in R using the package 'pheatmap'. The redundancy analysis (RDA) was carried out in R using the package 'vegan' to investigate the correlation of predicted microbial functions with the physicochemical properties.

3. RESULTS

3.1. Physicochemical properties

The pH value of the overlying water in all the samples exhibited a temporary decline before it began to increase consistently (Figure 2(a)). The lowest pH value in the control group was 7.47, while those in L, M, and H groups were 7.23, 6.91, and 6.58, respectively. The pH values in the voltage groups were lower than that in the control group during the entire experiment, with lower pH values at higher voltages. The EC values of the overlying water in all the groups exhibited a fluctuating decline, reaching minimum values of 784 μS/cm (control), 702.2 μS/cm (L), 598.7 μS/cm (M), and 593.1 μS/cm (H) on the 30th day. Similarly, the EC values in the voltage groups were lower than that in the control, and no further reduction in the EC values was observed after the applied voltage reached 5 V (Figure 2(b)).

The DO of the water column in the control group started increasing on the 12th day and reached the maximum value of 3.25 $mg{\cdot}L^{-1}$ on the 20th day. Subsequently, it exhibited a sharp decline and decreased to 0.81 $mg{\cdot}L^{-1}$ on the 28th day (Figure 2(c)). A similar trend was observed for the DO in the L group, with a maximum value of 2.29 $mg{\cdot}L^{-1}$ on the 24th day. In contrast, the DO in the M and H groups indicated a delayed but consistent increase on the 16th day, reaching the maximum values of 2.83 and 1.96 $mg{\cdot}L^{-1}$ at the end of the experiment, respectively. The ORP-W increased from -129.38 ± 24.30 to $+440.09 \pm 29.23$ mV, indicating that the oxidation conditions in the water column were improved. The maximum value of ORP-W was observed in the L group, followed by the control, H, and M groups (Figure 2(d)). The ORP-S in all the groups exhibited a fluctuating increase from -154.18 ± 16.94 to $+157.11 \pm 21.62$ mV (Figure 2(e)). Moreover, the ORP-S values exhibited significant inter-group differences (ANOVA: $p < 0.05$), with higher values observed in voltage treatments compared to the control group (mean value: L > M > H > control), indicating that voltage interventions are effective in improving the oxidation conditions of the surface sediment.

An increasing trend was observed for NH_4^+-N concentrations in all the groups during the early stages of the experiment, reaching the maximum values of 30.03, 31.29, 36.09, and 28.69 $mg{\cdot}L^{-1}$ in the control, L, M, and H groups, respectively. However, the concentration in the control group decreased sharply from 30.03 to 1.02 $mg{\cdot}L^{-1}$ in the later stages of the experiments, whereas it showed a slowly declining trend in the M and H groups. NH_4^+-N concentrations in the M and H groups decreased to 16.44 and 17.5 $mg{\cdot}L^{-1}$, respectively on the 50th day, which was still much higher than that in the control (Figure 2(f)).

The chroma in the control group increased to the maximum value (31.15) on the 7th day and then decreased to 5.22 on the 11th day. The chroma in the L group exhibited a similar trend, with a maximum value (42.85) slightly higher than that in the control. However, the chroma in the M group varied within a small range (0.75–11.58). The chroma in the H group rapidly increased to 62.93 and then gradually declined to 2.88 by the end of the experiment (Figure 2(g)). The turbidity of

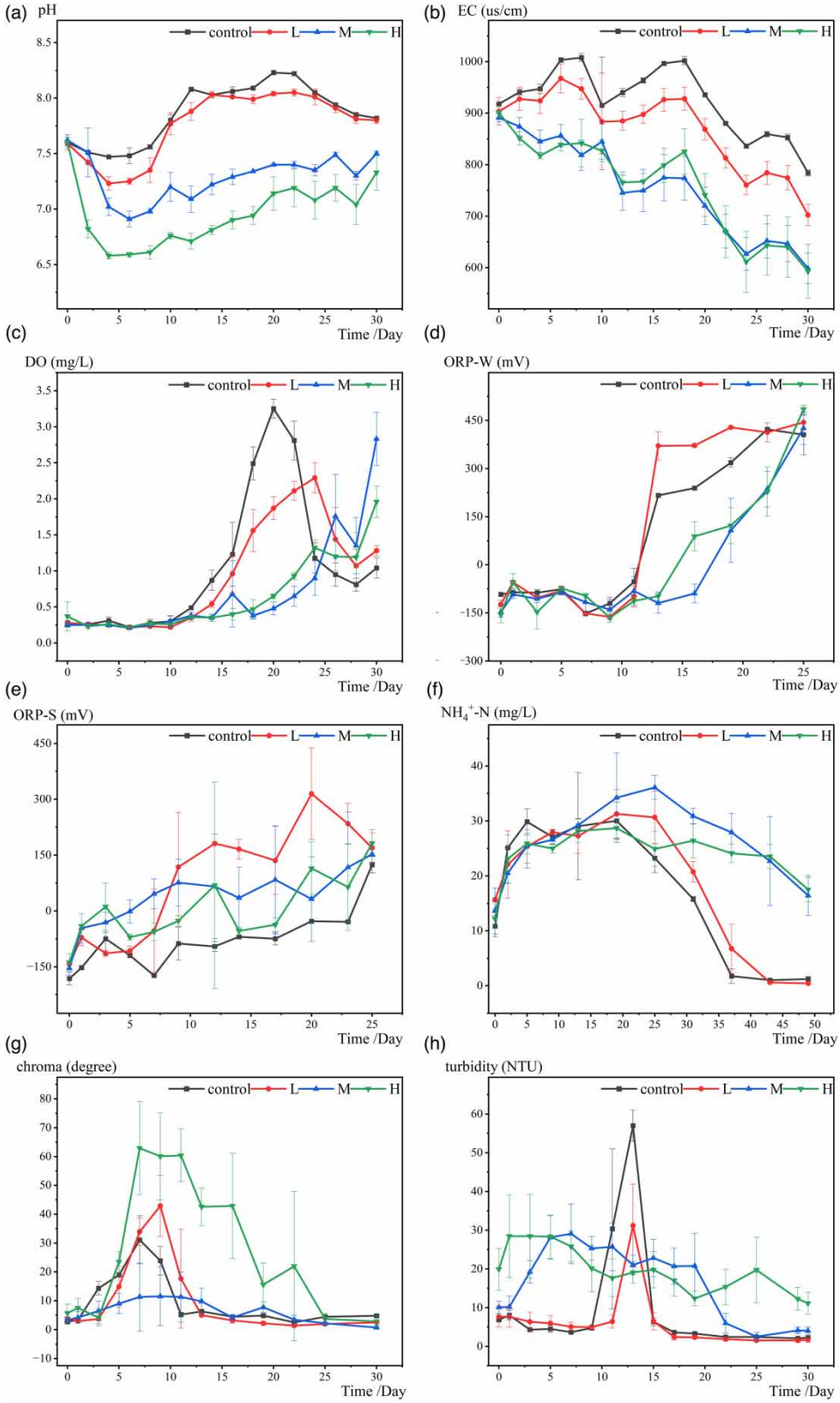

Figure 2 | Temporal variations in pH (a), EC (b), DO (c), ORP-W (d), ORP-S (e), NH_4^+-N (f), chroma (g), and turbidity (h) in various groups.

the water column in the control and L groups showed extreme values (57 and 31.18, respectively) around the 12th day. Except for these values, the turbidity in the M and H groups was significantly higher than that in the control (Figure 2(h)). The turbidity and chroma are used to describe the appearance of water, both of which were significantly higher in the H group.

3.2. Gas emissions

H_2S and NH_3 are the major sources of odors in black-odorous water (Song *et al.* 2017). CH_4 and CO_2 are organic decomposition products under anaerobic and aerobic conditions, respectively (Liu & Greaver 2009). H_2S, NH_3, and CH_4 are primarily produced under reductive conditions; therefore, the emission rates of all these three gases exhibited similar decreasing trends with improved oxidation conditions of black-odorous water. The results indicated that the emission rates of H_2S, NH_3, and CH_4 were lower while the emission rate of CO_2 was significantly higher in the M and H treatments when compared to those in the control (Figure 3). The emission rates of H_2S in the control and L groups showed a slight increase before it started to decline consistently, reaching the maximum values of 24.39 and 26.76 $\mu mol \cdot h^{-1}$, respectively. In contrast, the rates of H_2S in the M and H treatments exhibited a rapid decrease at the start of the experiment, reaching the maximum values of 16.45 and 19.98 $\mu mol \cdot h^{-1}$, respectively (Figure 3(a)). Similar trends were observed in the emission rates of NH_3 (Figure 3(b)) and CH_4 (Figure 3(c)). On the other hand, the emission rates of CO_2 in the voltage treatments were significantly higher than that in the control (Figure 3(d)). The average rate of CO_2 emissions in the control group was 77.83 $\mu mol \cdot h^{-1}$, while those in the L, M, and H groups were 85.83, 143.07, and 243.91 $\mu mol \cdot h^{-1}$, respectively. Furthermore, the total gas emissions were estimated based on the emission rates (Supplementary material, Table S3). The total emissions of H_2S, NH_3, and CH_4 in the H group were 38, 61, and 24% lower than those in the control, respectively. On the contrary, the total emission of CO_2 in the H group was up to 228% higher than that in the control. Briefly, voltage intervention can effectively inhibit the emissions of H_2S, NH_3, and CH_4 while enhancing the emission of CO_2, indicating that the sulfate reduction and organic degradation processes in the sediments might be affected.

3.3. Interstitial ions

Figure 4 shows the temporal variations in the interstitial SO_4^{2-} and NO_3^- concentrations, both of which can act as electron acceptors during anaerobic respiration (Gregory *et al.* 2004; Jin 2012). Previous studies have indicated that nitrate can effectively compete with sulfate for the substrate (Laverman *et al.* 2012). The ORP of the sulfate reduction process (−100 mV) was also much lower than that of the nitrate-reduction process (+400 mV) (Zhang *et al.* 2022). Therefore, interstitial SO_4^{2-} concentration was much higher than NO_3^- concentration in this study (Figure 4). The interstitial SO_4^{2-} concentration in the control group decreased from 116.75 to 103.23 $mg \cdot L^{-1}$ during the first period (0–10 days) and then increased to 196.11 $mg \cdot L^{-1}$ during the later period (10–30 days) (Figure 4(a)). On the contrary, the interstitial SO_4^{2-} concentration in the M and H groups did not decrease but slightly increased during the first period, which was consistent with the decreasing trend of H_2S emission rate during the same period (Figure 3(a)). Moreover, the subsequent increase in the interstitial SO_4^{2-} concentrations was insignificant in the M and H groups, further indicating that the voltage intervention affected the sulfur-related processes in sediments.

The interstitial NO_3^- concentration in the control group exhibited a slight decrease from 0.15 to 0.13 $mg \cdot L^{-1}$ during the early stage and consistently increased to 0.49 $mg \cdot L^{-1}$ with time during the later stage (Figure 4(b)). The interstitial NO_3^- concentration in the L group demonstrated a trend similar to that of the control. However, the interstitial NO_3^- concentrations in the M and H groups at the end of the experiment (0.17 and 0.20 $mg \cdot L^{-1}$, respectively) were significantly lower than that in the control (0.49 $mg \cdot L^{-1}$). Nitrates primarily originate from nitrification, an aerobic microbial process that involves the sequential oxidation of NH_4^+-N to NO_2^--N by ammonia-oxidizing bacteria (AOB) and NO_2^--N to NO_3^--N by nitrite-oxidizing bacteria (NOB). On the 20th day of the experiment, the higher DO levels in the control (3.25 mg/L) and L (1.87 mg/L) groups facilitated nitrification, the process by which NH_4^+-N is oxidized to NO_3^--N or NO_2^--N while oxygen is consumed. In contrast, the lower DO levels in the M (0.48 mg/L) and H (0.65 mg/L) groups hindered nitrification, resulting in a negligible increase in NO_3^- concentrations. Moreover, nitrates can serve as electron acceptors for microbial oxidation of organic pollutants under anaerobic conditions, a process known as nitrate reduction. The lower DO levels in the M and H groups favored nitrate reduction, which also contributed to the lower NO_3^- concentrations observed in these groups.

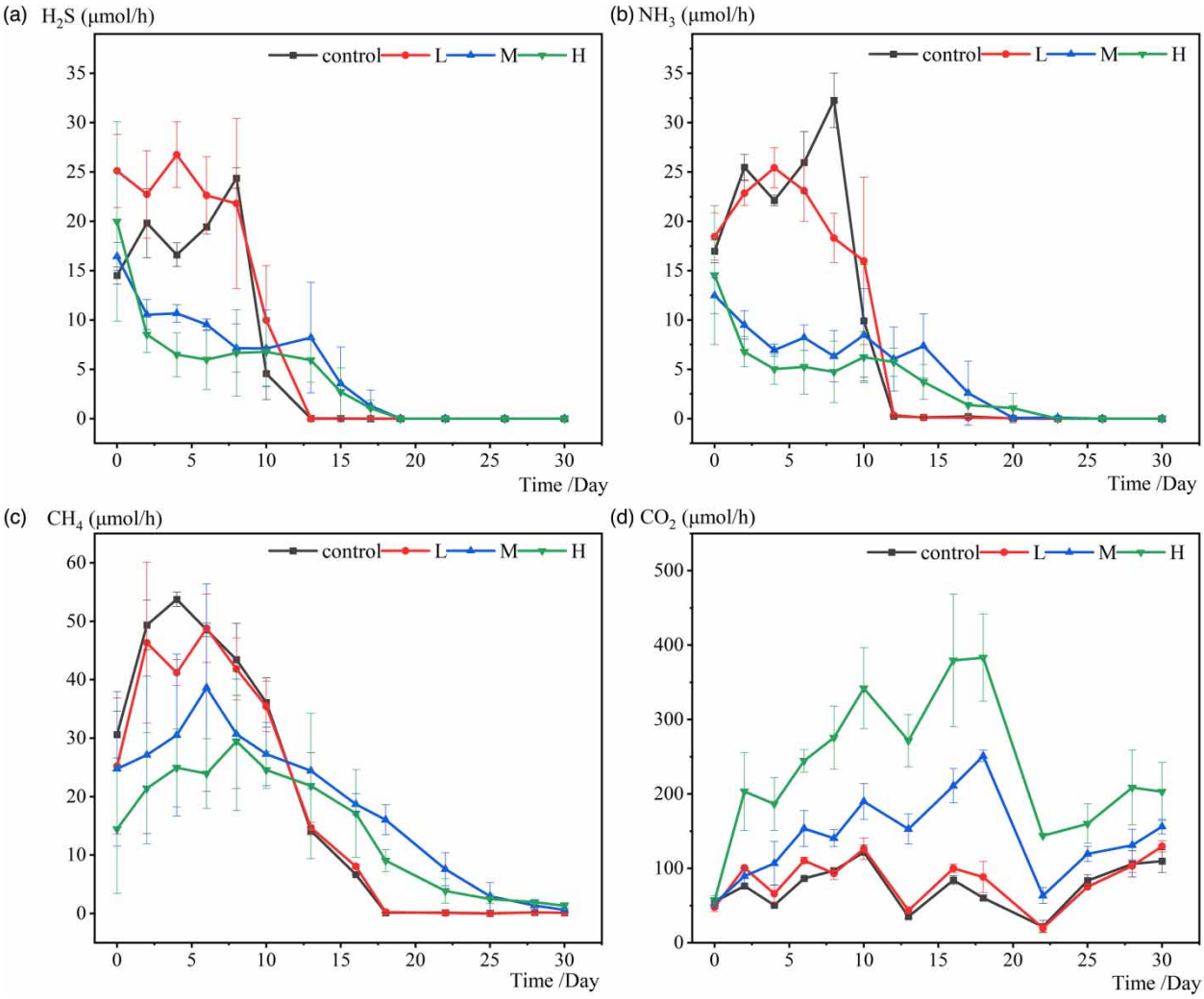

Figure 3 | Temporal variations in the emission rates of H_2S (a), NH_3 (b), CH_4 (c), and CO_2 (d) in various groups.

3.4. Microbial community diversity

A total of 864,701 effective sequences were obtained from 16 sediment samples using Illumina sequencing of 16S rRNA gene amplicon, with at least 47,401 effective sequences obtained in a single sample. A total of 5,603 ASVs were obtained by rarefication of the minimum number of effective sequences (47,401), which contained 30 bacterial and five archaeal phyla.

The species richness and microbial community diversity of each group increased with time during the remediation process of black-odorous water (Supplementary material, Figure S2). The highest ACE, Chao1, and Shannon indices were observed in the L group, followed by the control, M, and H groups. This indicated that low-voltage intervention might lead to an increase in the species richness and microbial community diversity, while high-voltage might lead to a decrease in these parameters. Furthermore, the change in the Shannon index was more significant than that in the Simpson index because the Shannon index gives greater weightage to the low-abundance species and is more susceptible to them (Dušek & Popelková 2017). Thus, it can be stated that the voltage interventions affected species richness and microbial community diversity primarily by affecting the low-abundance species and has little effect on the survival of the most abundant indigenous microorganisms.

PCA was performed using ASVs from 16 samples, which were divided into four groups according to different voltage treatments. The distribution of points in the control and L groups was more concentrated, while the points in the M and H groups were more scattered and different from the control (Supplementary material, Figure S3), indicating significant effects of voltage intervention on the microbial community at higher voltages.

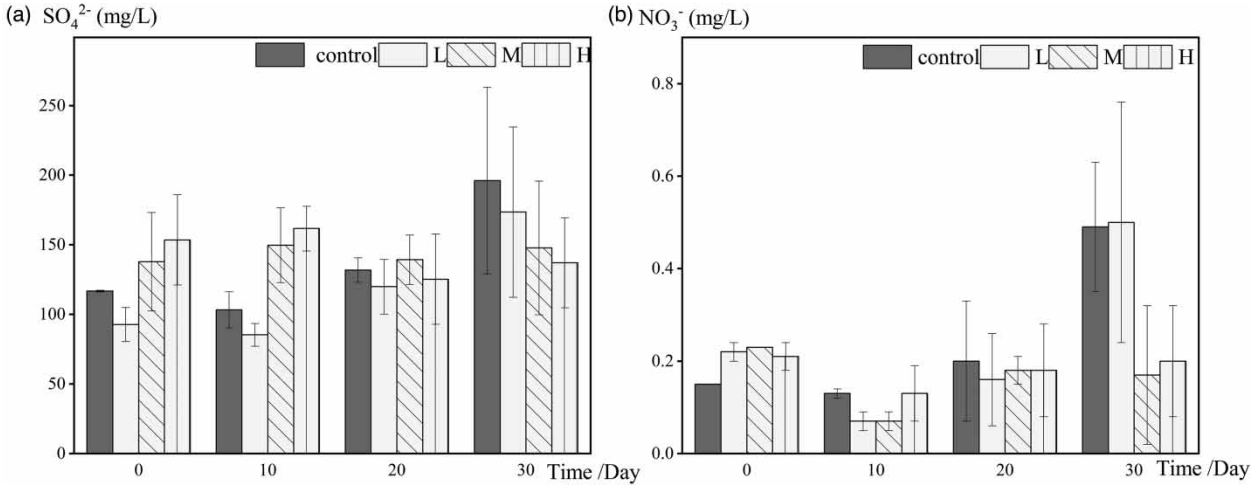

Figure 4 | Temporal variations in the interstitial water SO_4^{2-} (a) and NO_3^- (b) concentrations.

3.5. Microbial community structure

The major phyla in the sediments were Proteobacteria (24–52%), Firmicutes (18–42%), Desulfobacterota (10–15%), Bacteroidota (2–6%), Verrucomicrobiota (1–9%), and Halobacterota (1–6%) (Figure 4(a)). Proteobacteria were the most dominant phylum in almost all the samples. The average relative abundance of Proteobacteria in the control group was 36.8%, while those in the voltage treatments were 33.6, 41.4, and 44.1% for L, M, and H groups, respectively. In contrast, the average relative abundance of Desulfobacterota in the control group was 12.1%, slightly higher than that in the H group (10.6%). Furthermore, the relative abundance of Halobacterota was slightly lower in the M (3.2%) and H (1.7%) voltage treatments than that in the control (4.3%). Overall, the microbial community structures at the phylum level indicated that there was an increase in the relative abundance of Proteobacteria and a decrease in those of Desulfobacterota and Halobacterota at a voltage of 10 V.

At the genus level, 605 genera were identified in 16 samples. *Dechloromonas*, *Desulfovirga*, and *Symbiobacterium* were the top three abundant genera, followed by *Citrifermentans*, *Azospira*, *Azospirillum*, *Sedimentibacter*, *Zoogloea*, *Methobanolus*, *Lysobacter*, and *Thiobacillus* (Supplementary material, Figure S4). The clustering network analysis was performed by Cytoscape to elucidate the differences among the four groups. *Dechloromonas* was the most abundant genus, accounting for a larger proportion in the M and H groups. Similarly, the genera *Azospira*, *Azospirillum*, and *Pannonibacter* were relatively more abundant in the M and H treatments (Figure 4(b)). On the contrary, the relative abundances of *Desulfovirga*, *Symbiobacterium*, *Methanolobus*, and *Thiobacillus* in the M and H groups were lower than those in the control. In addition, some species with lower abundance also demonstrated significant differences. *Prosthecobacter* was unique in the control group. The relative abundance of *Zoogloea* in the L group was significantly higher than that in the other three groups. The highest abundance of *Methylotenera* was observed in the M group, while *Comamonas*, *Clostridium-sensu-stricto-7*, and *Cloacibacterium* were predominant in the H group.

3.6. Predicted microbial functions by FAPROTAX

FAPROTAX analysis was performed to investigate the effects of voltage intervention on the potential microbial functions in the sediments. The functional processes that dominated the sediments included chemoheterotrophy, nitrate reduction, sulfate reduction, nitrogen fixation, fermentation, ureolysis, dark iron-oxidation, dark oxidation of sulfur compounds, nitrite reduction, chitinolysis, methanogenesis, and phototrophy (Figure 6(a)). It was predicted that sulfate reduction, dark oxidation of sulfur compounds, and phototrophy functions were relatively more abundant in the control group, while chemoheterotrophy, nitrate reduction, nitrogen fixation, ureolysis, and dark iron-oxidation were predominant in the M and H groups (Figure 6(b)). Moreover, the relative abundance of methanogenesis in the H group was the lowest among the four groups. Furthermore, the PCA was also applied to analyze the similarity of the microbial functions among different samples, using

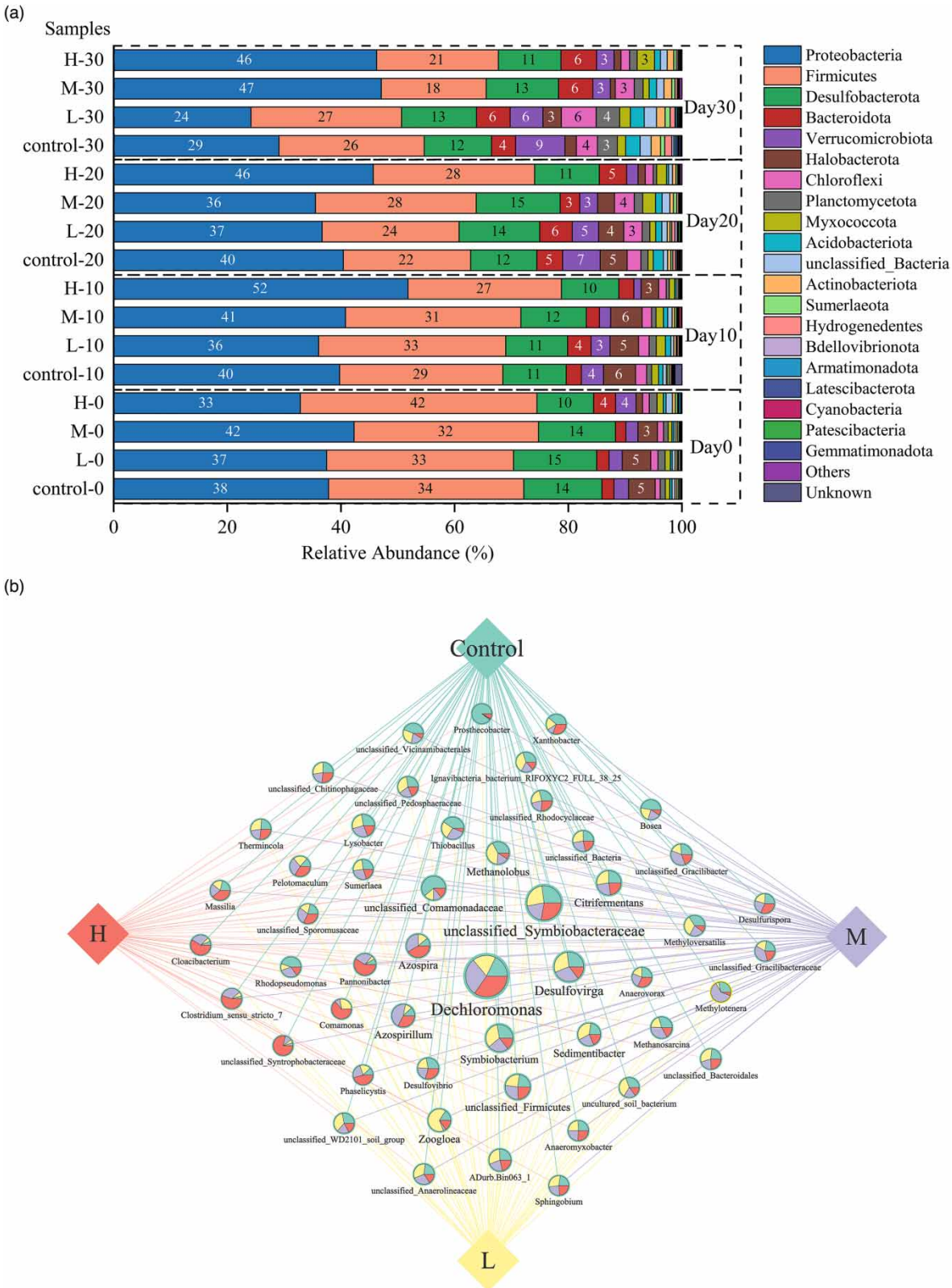

Figure 5 | (a) Relative abundance of major phyla in 16 samples; (b) profile clustering using the Cytoscape network visualizes the top 50 abundant genera across four groups. The pie chart of the node sizes represents the relative abundance of the genus in the respective groups.

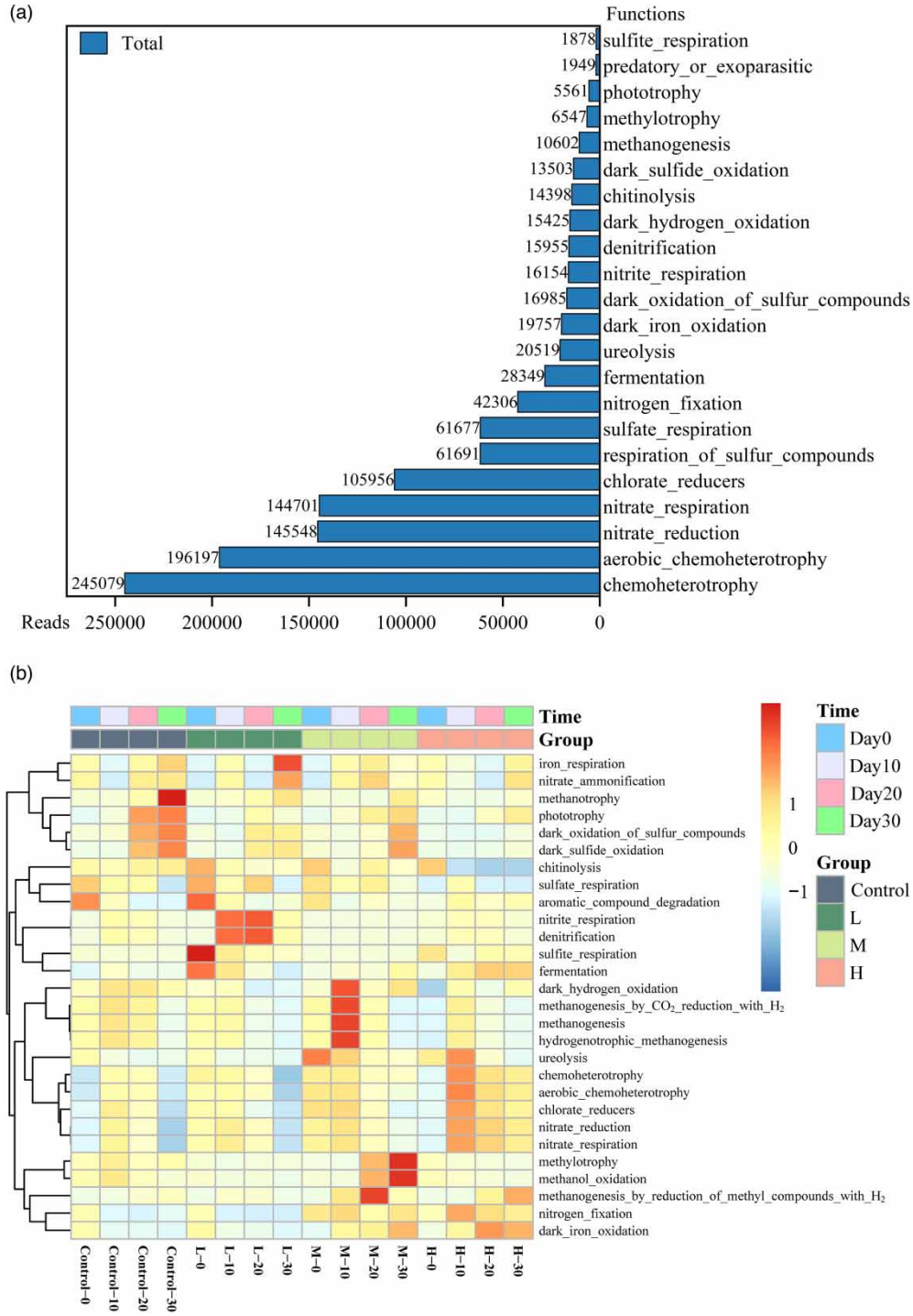

Figure 6 | (a) Total reads of dominant predicted functions in all the samples and (b) clustering heatmap of predicted functions. Functional predictions and functional classifications were based on the functional annotation of prokaryotic taxa (FAPROTAX).

the number of reads for each predicted function (Supplementary material, Figure S5). The results indicated that the distribution of points in the M and H groups were more concentrated, while the points in the L group were more dispersed, which demonstrated that the voltage interventions of 5 and 10 V might enhance the selectivity of the environment, thereby leading to concentrated microbial functions.

4. DISCUSSION

4.1. Correlation analysis of physicochemical properties

Correlation analysis was performed to analyze the relationship among all the physicochemical properties (Figure 7(a)). pH showed a significant negative correlation with emission rate of CO_2 ($r = -0.74$, $p \leq 0.01$). ORP-W indicated significant positive correlations with DO ($r = +0.86$, $p \leq 0.001$) and ORP-S ($r = +0.74$, $p \leq 0.01$), while negative correlations with the emission rates of CH_4 ($r = -0.92$, $p \leq 0.001$), H_2S ($r = -0.74$, $p \leq 0.01$), and NH_3 ($r = -0.85$, $p \leq 0.001$). This can be explained by the fact that all these gases were mainly produced under anaerobic conditions. However, sulfate concentrations were not significantly correlated with H_2S emission rates ($r = -0.37$, $p = 0.16$), indicating that H_2S was emitted not only from the sulfate reduction process but also from the anaerobic degradation of sulfur-containing proteins, such as methionine.

4.2. Relationships between the physicochemical properties and predicted microbial functions

The relationships between the physicochemical properties and the relative abundances of predicted microbial functions were analyzed by RDA (Figure 7(b)). The emission rate of H_2S was positively correlated with the relative abundances of aromatic compound degradation, sulfate reduction, and sulfite reduction functions, while negatively correlated with sulfate concentration and the relative abundance of dark oxidation of sulfur compounds. These relationships corroborated that the H_2S emission in this study were mainly from the anaerobic degradation of sulfur-containing organics and sulfate reduction. Moreover, the emission rate of CH_4 was positively correlated with methanogenesis, while negatively correlated with methanotrophy and phototrophy. This was because enhanced phototrophy function was generally accompanied by increased oxygen production and ORP, which would lead to the inhibition of methanogenic activities under anaerobic conditions. Furthermore, the emission rate of CO_2 was positively correlated with chemoheterotrophy, indicating that CO_2 emission might be partly enhanced due to the activities and respiration of chemoheterotrophic bacteria in the sediments. In addition, the nitrate concentration demonstrated a negative correlation with the relative abundance of nitrate reduction, which explained that the lower nitrate concentrations in the M and H groups were partially due to the enhanced nitrate reduction functions. Generally, it can be stated that the voltage interventions significantly affected the potential microbial functions involved in S, C, and N element cycles, which further affected the physicochemical environment and gas emissions in black-odorous water.

4.3. Effects of voltage intervention on the water quality

The results indicated that the voltage interventions significantly affected the physicochemical properties of black-odorous water. Firstly, the oxidative conditions in the surface sediments were effectively improved upon application of the voltages. The anode electrode placed on the sediment surface can aid in the oxidation of reductive gases and pollutants, thereby improving ORP-S (Moreira *et al.* 2017). Meanwhile, the electric field induces the discharge of water to produce hydroxyl radicals with strong oxidation capacity, which can oxidize reductive substances such as H_2S, NH_3, CH_4, and organic pollutants (Panizza & Cerisola 2009). The ORP-S values are influenced by both the anode electrode and the redox environment of the overlying water. However, the experimental results suggest that the voltage groups did not exhibit a significant increase in DO or ORP-W levels, and in fact, they were lower than those in the control group. This finding suggests that the electrode could not effectively generate O_2 through water electrolysis. Moreover, the cathode electrode placed on the water surface can lead to the cathodic reduction of oxygen at voltages of 5 V and above, thus affecting the reoxygenation efficiency and leading to delayed improvements in DO and ORP-W (Kaneko *et al.* 2006). Considering the mutual influence of the sediment and the overlying water, this can further lead to a decrease in ORP-S. Therefore, the improvement effect of voltage interventions on the ORP-S did not increase with higher voltages, as the highest ORP-S value was observed in the L group (Figure 2(e)).

In the voltage treatments, pH continued to decrease with an increase in voltage, partly due to the oxidation of H_2S to more acidic H_2SO_4 or H_2SO_3 near the anode. Meanwhile, H^+ was also produced during the oxidation of organics by the hydroxyl radicals (Panizza & Cerisola 2009), which was corroborated by the significant negative correlation between pH and CO_2 emission rate (Figure 7(a)). Moreover, the intermittent existence of the electric field was not conductive to the settling of suspended matter, while augmented gas emissions also added hydrodynamic disturbances, ultimately resulting in increased chroma and turbidity of the water column.

Briefly, these results had illustrated that voltage intervention could be effective in increasing ORP-S and inhibiting the emissions of reductive odors such as H_2S, NH_3, and CH_4. However, the water disturbance caused by the electrodes

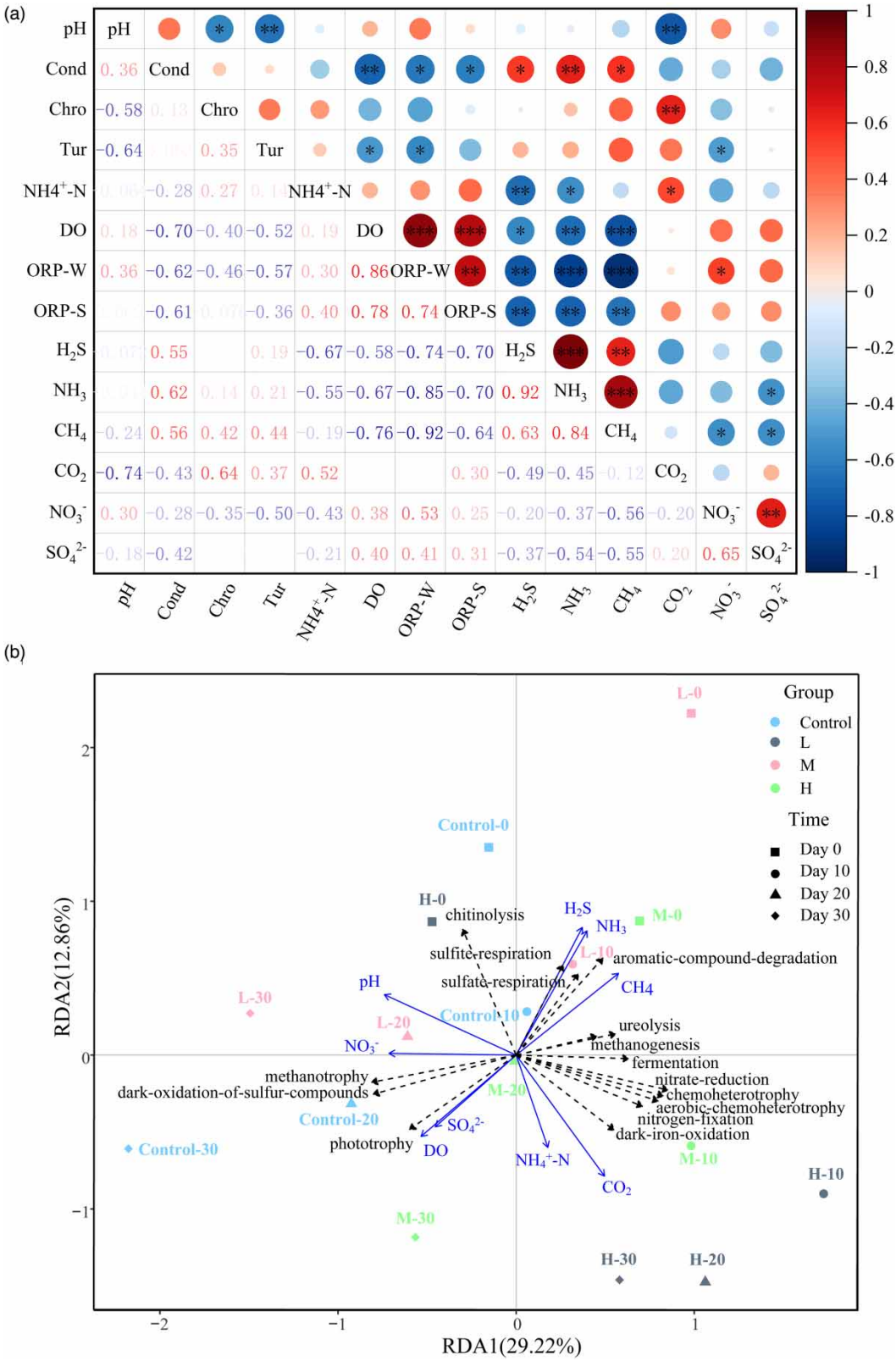

Figure 7 | (a) Correlation analysis of different physicochemical properties (the number marked in the figure represents the correlation coefficient; the color intensity indicates correlation strength; significant difference was denoted with $***p < 0.001$, $**p < 0.01$, $*p < 0.05$) and (b) redundancy analysis (RDA) of correlation between physicochemical properties and potential microbial functions.

and gas emissions could lead to an increase in the chroma and turbidity of the water column. Meanwhile, the cathodes could lead to delayed improvements in DO and ORP in the overlying water.

4.4. Effects of voltage intervention on the gas emission processes

The results indicated that the voltage interventions of 5 and 10 V inhibited the emissions of H_2S, NH_3 and CH_4 while significantly enhancing the emission of CO_2 (Figure 3). As mentioned in Section 4.2, NH_3 and H_2S emitted from the reactors mainly came from sulfate reduction and degradation of sulfur-containing organics. It has not yet been confirmed that electron acceptors have an inhibitory effect on the mineralization of organic sulfur compounds. No significant difference was observed in the variations of NH_4^+-N concentrations between the control and voltage treatments during the early experimental period (Figure 2(f)), indicating that voltage intervention had a minimal effect on the decomposition of methionine. However, SRBs are generally considered strict anaerobic microorganisms. Prior studies have shown that the metabolism of sulfate-reducing microorganisms is hindered when the ORP exceeds −100 mV (Zhang *et al.* 2022). Consequently, the increased ORP-S would impede the activities of SRB, leading to a reduction in H_2S emission rates in the voltage treatments. *Desulfovirga* is a typical SRB that can reduce SO_4^{2-}, SO_3^{2-}, or $S_2O_3^{2-}$ to H_2S using a variety of organics as electron donors (Davidova *et al.* 2022). The lowest abundance of *Desulfovirga* was observed in the H group, which was in agreement with the low abundance of sulfate reduction and sulfite reduction functions in this group (Figure 6(b)). On the contrary, the genera *Dechlormonas* and *Azospira*, which were generally considered perchlorate-reducing or nitrate-reducing microorganisms, were significantly predominant in voltage groups (Chakraborty & Picardal 2013). Previous studies have demonstrated that all the known dissimilatory perchlorate-reducing microorganisms are naturally able to oxidize H_2S (Mehta-Kolte *et al.* 2017). In addition, the electrogenerated hydroxyl radicals can oxidize H_2S and NH_3 in the water column, which also leads to a decline in their emission rates.

The effects of voltage interventions on CH_4 emission were similar to those on H_2S emission. On the one hand, the increase in ORP-S inhibited the methanogenesis process in sediments. *Methanolobus* and *Methanosarcina* were the predominant methanogens in the sediments (Supplementary material, Figure S4), both of which can utilize a range of substrates for methanogenic activities even in extreme environment (Gao *et al.* 2017). The lowest abundances of both *Methanolobus* and *Methanosarcina* were observed in the H group (Figure 5(b)), indicating that voltage intervention of 10 V was detrimental to the survival and activities of methanogens. Accordingly, the lowest relative abundance of predicted methanogenesis function was observed in the H group (Figure 6(b)), which was consistent with the lowest CH_4 emission rate observed in this group (Figure 3(c)). Furthermore, CH_4 can be oxidized into CO_2 by hydroxyl radicals, which also leads to a decrease in the CH_4 emission rate.

CO_2 is the product of the oxidative decomposition of organics and CH_4 oxidation. In this study, the emission rate of CO_2 was much higher than that of CH_4 (Figure 3), indicating that other sources were also responsible for increased CO_2 emission apart from CH_4 oxidation. The function prediction results indicated that the chemoheterotrophy and nitrate reduction functions in sediments were significantly enhanced with an increase in the voltage (Figure 6(b)). Moreover, the RDA results implied that the emission rate of CO_2 was positively associated with the microbial chemoheterotrophic activities (Figure 7(b)). The chemoheterotrophic microorganisms, such as *Dechloromonas*, *Azospira*, *Azospirillum*, and *Pannonibacter*, displayed higher relative abundances in the M and H groups (Figure 5(b)), potentially resulting from decreased competition for resources as a consequence of reduced relative abundances of SRB and methanogens in response to environmental changes. These microorganisms are critical contributors to the anaerobic decomposition of organic matter. Most species of *Dechloromonas* can grow anaerobically by coupled processes involving complete oxidation of organic acid and chlorate reduction, where nitrate can also serve as the sole electron acceptor (Chakraborty & Picardal 2013). *Azospirillum* is usually known as a nitrogen-fixing bacterium, which is widely used in agriculture for promoting plant growth (Cassán *et al.* 2020). Perez-Garcia *et al.* (2010) have demonstrated that the addition of *Azospirillum* had a positive effect on the nitrogen and phosphorus uptake by *Chlorella* under light conditions, and it has been applied in wastewater treatment. *Pannonibacter* was usually applied in aromatic compound degradation and nitrogen removal in previous studies (Bai *et al.* 2019). Therefore, the increased relative abundances of these microorganisms actually indicated the improved biochemical degradability of sediments. In addition, the hydroxyl oxidation of both organics and CH_4 also contributed to CO_2 emission.

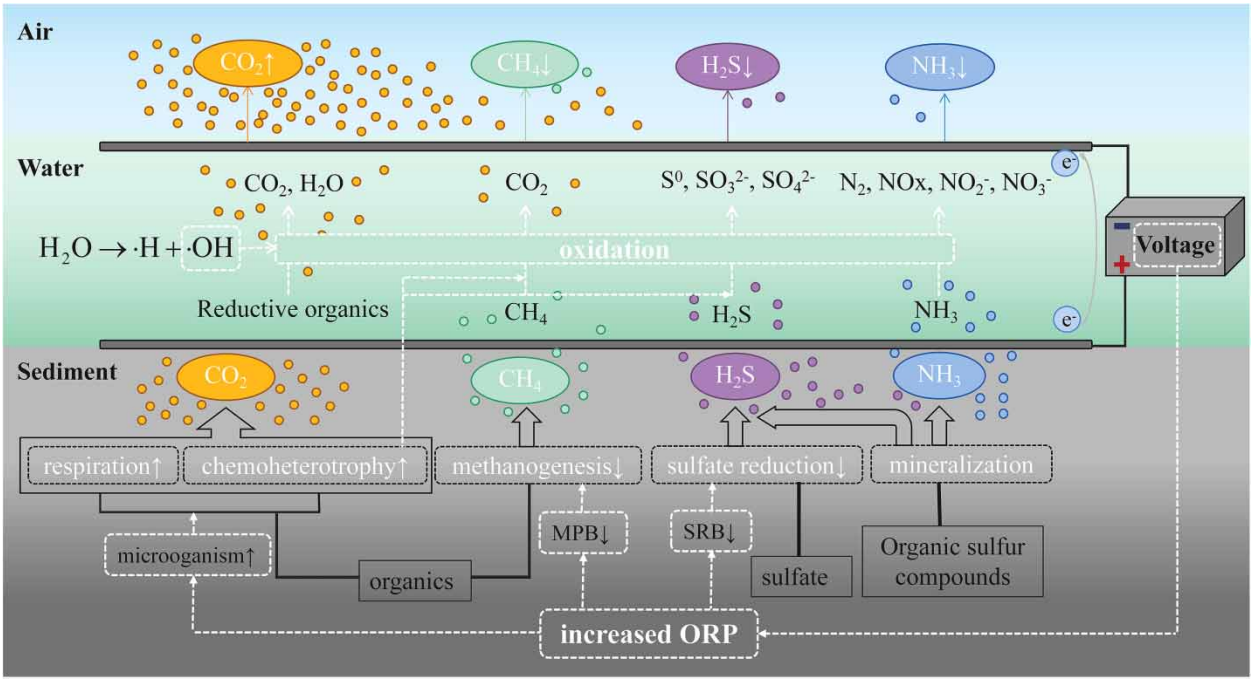

Figure 8 | Mechanisms underlying the effects of voltage intervention on gas emissions from black-odorous water and sediments.

Briefly, voltage intervention can effectively promote the complete decomposition of organics and inhibit the emission of reductive odor gases. The mechanisms underlying the effects of voltage intervention on the gas emissions from black-odorous water and sediments are summarized in Figure 8.

5. CONCLUSION

In this study, the effects of voltage interventions of 2.5, 5, and 10 V on the remediation of black-odorous water were investigated by conducting simulation experiments. The voltage interventions of 5 and 10 V can effectively increase the ORP of the surface sediments and inhibit the emissions of reductive odor gases such as H_2S, NH_3, and CH_4. On the contrary, the emission of CO_2 was significantly enhanced after voltage treatments. Moreover, voltage interventions have a significant effect on the microbial activities in the sediments. The relative abundances of typical methanogens (*Methanosarcina* and *Methanolobus*) and SRB (*Desulfovirga*) decreased while the chemoheterotrophic microorganisms (e.g., *Dechloromonas*, *Azospira*, *Azospirillum*, and *Pannonibacter*), which play important roles in the anaerobic oxidative decomposition of organics, became more abundant. Meanwhile, voltage application also led to a significant enhancement in the predicted microbial chemoheterotrophy and nitrate reduction functions in the sediments, implying the improved biochemical degradability of sediments.

In summary, the results demonstrated that electrochemical remediation of black-odorous water is feasible and the implementation effect is significant. The oxidation conditions in the sediments were improved and the water odor was effectively eliminated after voltage treatments. The findings of this research provide insights into the electrochemical treatment of black-odorous water. However, further research is still needed to avoid the adverse effects of voltage devices, such as water disturbance and impeded reoxygenation processes.

ACKNOWLEDGEMENTS

This work has been jointly supported by the National Natural Science Foundation of China (No. 42077221), the Fundamental Research Funds for the Central Universities (No. 2019B72714), the Postgraduate Research and Practice Innovation Program of Jiangsu Province (No. SJKY19_0472).

AUTHOR CONTRIBUTIONS

Y.S. conceptualized the study, did data curation, did formal analysis, investigated the study, performed methodology, visualized the study, and wrote the original draft. Z.W. did formal analysis, performed methodology, supervised the study, wrote, reviewed, and edited, and did project administration. Y.X. performed the methodology, supervised the study, wrote, reviewed and edited the article, and did project administration. X.L. did formal analysis, supervised the study, wrote, reviewed, and edited the article, and did project administration. A.R. supervised the study, wrote, reviewed, and edited the article, and did project administration.

DATA AVAILABILITY STATEMENT

All relevant data are included in the paper or its Supplementary Information.

CONFLICT OF INTEREST

The authors declare there is no conflict.

REFERENCES

Bai, H., Liao, S., Wang, A., Huang, J., Shu, W. & Ye, J. 2019 High-efficiency inorganic nitrogen removal by newly isolated Pannonibacter phragmitetus B1. *Bioresource Technology* **271**, 91–99.

Callahan, B. J., McMurdie, P. J. & Holmes, S. P. 2017 Exact sequence variants should replace operational taxonomic units in marker-gene data analysis. *The ISME Journal* **11** (12), 2639–2643.

Cao, J., Sun, Q., Zhao, D., Xu, M., Shen, Q., Wang, D., Wang, Y. & Ding, S. 2020 A critical review of the appearance of black-odorous waterbodies in China and treatment methods. *Journal of Hazardous Materials* **385**, 121511.

Cassán, F., Coniglio, A., López, G., Molina, R., Nievas, S., de Carlan, C. L. N., Donadio, F., Torres, D., Rosas, S., Pedrosa, F. O., de Souza, E., Zorita, M. D., De-Bashan, L. & Mora, V. 2020 Everything you must know about Azospirillum and its impact on agriculture and beyond. *Biology and Fertility of Soils* **56** (4), 461–479.

Chakraborty, A. & Picardal, F. 2013 Neutrophilic, nitrate-dependent, Fe(II) oxidation by a Dechloromonas species. *World Journal of Microbiology and Biotechnology* **29** (4), 617–623.

Chen, C., Yang, X., Luo, H., Zeng, D., Sima, M. & Huang, S. 2020 Linking microbial community and biological functions to redox potential during black-odor river sediment remediation. *Environmental Science and Pollution Research* **27** (32), 40392–40404.

Chen, C., Yang, F., Deng, Y. & D, A. 2022 Optimization of constructed wetlands on purifying black-odorous water and their potential purification mechanism. *Water Science and Technology* **86** (9), 2175–2183.

Davidova, I. A., Duncan, K. E., Wiley, G. & Najar, F. Z. 2022 Desulfoferrobacter suflitae gen. nov., sp. nov., a novel sulphate-reducing bacterium in the Deltaproteobacteria capable of autotrophic growth with hydrogen or elemental iron. *International Journal of Systematic and Evolutionary Microbiology* **72** (8), 005483.

Dušek, R. & Popelková, R. 2017 Theoretical view of the Shannon index in the evaluation of landscape diversity. *Acta Universitatis Carolinae. Geographica* **47** (2), 5–13.

Gao, Y., Sun, D., Dang, Y., Lei, Y., Ji, J., Lv, T., Bian, R., Xiao, Z., Yan, L. & Holmes, D. E. 2017 Enhancing biomethanogenic treatment of fresh incineration leachate using single chambered microbial electrolysis cells. *Bioresource Technology* **231**, 129–137.

Gollnisch, R., Alling, T., Stockenreiter, M., Ahrén, D., Grabowska, M. & Rengefors, K. 2021 Calcium and pH interaction limits bloom formation and expansion of a nuisance microalga. *Limnology and Oceanography* **66** (9), 3523–3534.

Gregory, K. B., Bond, D. R. & Lovley, D. R. 2004 Graphite electrodes as electron donors for anaerobic respiration. *Environmental Microbiology* **6** (6), 596–604.

Jin, Q. 2012 Energy conservation of anaerobic respiration. *American Journal of Science* **312** (6), 573–628.

Kaneko, M., Nemoto, J., Ueno, H., Gokan, N., Ohnuki, K., Horikawa, M., Saito, R. & Shibata, T. 2006 Photoelectrochemical reaction of biomass and bio-related compounds with nanoporous TiO_2 film photoanode and O_2-reducing cathode. *Electrochemistry Communications* **8** (2), 336–340.

Laverman, A. M., Pallud, C., Abell, J. & Cappellen, P. V. 2012 Comparative survey of potential nitrate and sulfate reduction rates in aquatic sediments. *Geochimica et Cosmochimica Acta* **77**, 474–488.

Liu, L. & Greaver, T. L. 2009 A review of nitrogen enrichment effects on three biogenic GHGs: the CO_2 sink may be largely offset by stimulated N_2O and CH_4 emission. *Ecology Letters* **12** (10), 1103–1117.

Liu, C., Shen, Q., Zhou, Q., Fan, C. & Shao, S. 2015 Precontrol of algae-induced black blooms through sediment dredging at appropriate depth in a typical eutrophic shallow lake. *Ecological Engineering* **77**, 139–145.

Liu, X., Tao, Y., Zhou, K., Zhang, Q., Chen, G. & Zhang, X. 2016 Effect of water quality improvement on the remediation of river sediment due to the addition of calcium nitrate. *Science of The Total Environment* **575**, 887–894.

Lu, X., Feng, Z., Shang, J., Fan, C. & Deng, J. 2012 Black water bloom induced by different types of organic matters and forming mechanisms of major odorous compounds. *Environmental Science* **33** (09), 3152–3159.

Mehta-Kolte, M. G., Loutey, D., Wang, O., Youngblut, M. D., Hubbard, C. G., Wetmore, K. M., Conrad, M. E. & Coates, J. D. 2017 Mechanism of H_2S oxidation by the dissimilatory perchlorate-reducing microorganism Azospira suillum PS. *MBio* **8** (1), e02023-16.

Moreira, F. C., Boaventura, R. A. R., Brillas, E. & Vilar, V. J. P. 2017 Electrochemical advanced oxidation processes: a review on their application to synthetic and real wastewaters. *Applied Catalysis B: Environmental* **202**, 217–261.

Pan, M., Zhao, J., Zhen, S., Heng, S. & Wu, J. 2016 Effects of the combination of aeration and biofilm technology on transformation of nitrogen in black-odor river. *Water Science and Technology* **74** (3), 655–662.

Panizza, M. & Cerisola, G. 2009 Direct and mediated anodic oxidation of organic pollutants. *Chemical Reviews* **109** (12), 6541–6569.

Perez-Garcia, O., De-Bashan, L. E., Hernandez, J. & Bashan, Y. 2010 Efficiency of growth and nutrient uptake from wastewater by heterotrophic, autotrophic, and mixotrophic cultivation of chlorella vulgaris immobilized with azospirillum brasilense1. *Journal of Phycology* **46** (4), 800–812.

Song, C., Liu, X., Song, Y., Liu, R., Gao, H., Han, L. & Peng, J. 2017 Key blackening and stinking pollutants in Dongsha River of Beijing: spatial distribution and source identification. *Journal of Environmental Management* **200**, 335–346.

Wang, G., Li, X., Fang, Y. & Huang, R. 2014 Analysis on the formation condition of the algae-induced odorous black water agglomerate. *Saudi Journal of Biological Sciences* **21** (6), 597–604.

Watson, S. B. 2003 Cyanobacterial and eukaryotic algal odour compounds: signals or by-products? A review of their biological activity. *Phycologia (Oxford)* **42** (4), 332–350.

Yuan, Q., Shen, Y., Huang, Y. & Hu, N. 2018 A comparative study of aeration, biostimulation and bioaugmentation in contaminated urban river purification. *Environmental Technology & Innovation* **11**, 276–285.

Zhang, R., Zhao, X., Li, Q., Wei, J. & Li, Z. 2019 Research and application progress of electrochemical technology in wastewater treatment. *Technology of Water Treatment* **45** (4), 11–16.

Zhang, Z., Zhang, C., Yang, Y., Zhang, Z., Tang, Y., Su, P. & Lin, Z. 2022 A review of sulfate-reducing bacteria: metabolism, influencing factors and application in wastewater treatment. *Journal of Cleaner Production* **376**, 134109.

First received 26 January 2023; accepted in revised form 21 May 2023. Available online 31 May 2023